Observation of the Zero Doppler Effect.

Ran, J; Zhang, Y; Chen, X; Fang, K; Zhao, J; Chen, H

2016. Nature Publications

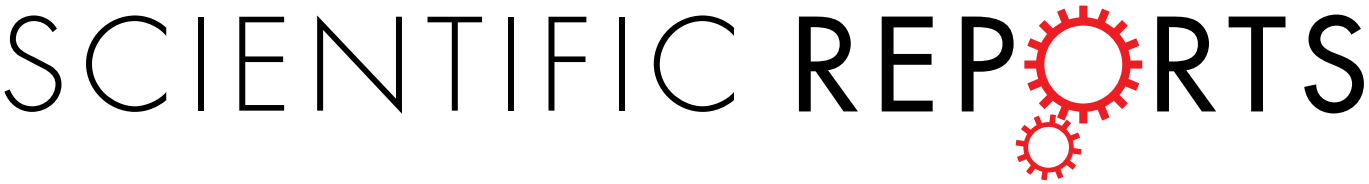

OPEN

Observation of the Zero Doppler Effect

Jia Ran[1,3], Yewen Zhang[1], Xiaodong Chen[2,3], Kai Fang[1], Junfei Zhao[1] & Hong Chen[1]

Received: 08 January 2016
Accepted: 16 March 2016
Published: 05 April 2016

The normal Doppler effect has well-established applications in many areas of science and technology. Recently, a few experimental demonstrations of the inverse Doppler effect have begun to appear in negative-index metamaterials. Here we report an experimental observation of the zero Doppler effect, that is, no frequency shift irrespective of the relative motion between the wave signal source and the detector in a zero-index metamaterial. This unique phenomenon, accompanied by the normal and inverse Doppler effects, is generated by reflecting a wave from a moving discontinuity in a composite right/left-handed transmission line loaded with varactors when operating in the near zero-index passband, or the right/left-handed passband. This work has revealed a complete picture of the Doppler effect in metamaterials and may lead to potential applications in electromagnetic wave related metrology.

The Doppler effect is a common phenomenon that the relative motion between a source and the detector causes a frequency shift in the received wave signal. In our daily life experience, i.e. in the normal dispersion media with both positive permittivity ε and permeability μ, an approaching source increases the received signal frequency, whereas a receding source decreases it.

Recently, the inverse Doppler effect, that the frequency decreases when the source is approaching the detector whereas increases when it is leaving the detector[1], was experimentally demonstrated by Seddon and Bearpark[2] and others[3–9] in the so-called left-handed (LH) metamaterials[10–17]. The mechanism for this abnormal phenomenon is that the group velocity and phase velocity are anti-parallel in such left-handed materials, deriving from that the permittivity ε and permeability μ are both negative (double negative materials, DNG). The rotational Doppler effect in left-handed metamaterials is also discussed in ref. 18.

A natural question is whether we can find a medium in which the zero Doppler effect, that is, no frequency shift irrespective of the relative motion between the source and the detector, can be observed experimentally. This question has motivated us to study the Doppler effect in a metamaterial with both permittivity and permeability near zero, referred as (near) zero-index metamaterial (ZIM)[19–24]. It is demonstrated that the wave phase velocity is infinite while there is still electromagnetic (EM) wave transfer inside the zero-index metamaterial[25,26], as shown in Supplementary Movie 1.

We have realized the zero-index metamaterial on a tunable composite right/left-handed transmission line (CRLH TL)[26–29] loaded with varactors[3,30]. The constructed CRLH TL exhibits in turn a left-handed passband, a stopband and a right-handed (RH) passband over the operating frequency band[27,28]. By choosing the proper component parameters on the CRLH TL (see details in Methods), the stopband can be narrowed down to vanish at a frequency at which both permeability and permittivity are near zero, referred as a balanced CRLH TL[17]. Hence, the (near) zero-index metamaterial is obtained at this frequency.

In order to conduct the Doppler effect experiment, we need to apply different bias voltages on the varactor loaded on the CRLH TL to switch the transmission characteristics of the CRLH transmission units between the (near) zero-index passband and a stopband by a digital circuit referred as the reflective interface controller[3]. In our Doppler effect experiments, instead of moving the source or the detector, we have created a moving interface to reflect the incoming RF signal. The reflective interface is formed by setting the left section of CLRH TL units in passband and the right section of units in band gap (stopband). When switching the transmission characteristic of the unit next to the reflective interface from band gap to passband, the reflective interface can be moved one unit rightward. Switching the transmission characteristics of the units next to the reflective interface in succession, a moving reflective interface can be achieved on the transmission line. The reflective interface could be considered moving successively when the wavelength is considerably larger than the length of the transmission

[1]Tongji University, Shanghai, 200092, China. [2]University of Electronic Science and Technology of China, Chengdu, 610054, China. [3]Queen Mary University of London, E1 4NS, UK. Correspondence and requests for materials should be addressed to Y.Z. (email: yewen.zhang@tongji.edu.cn) or X.C. (email: xiaodong.chen@qmul.ac.uk)

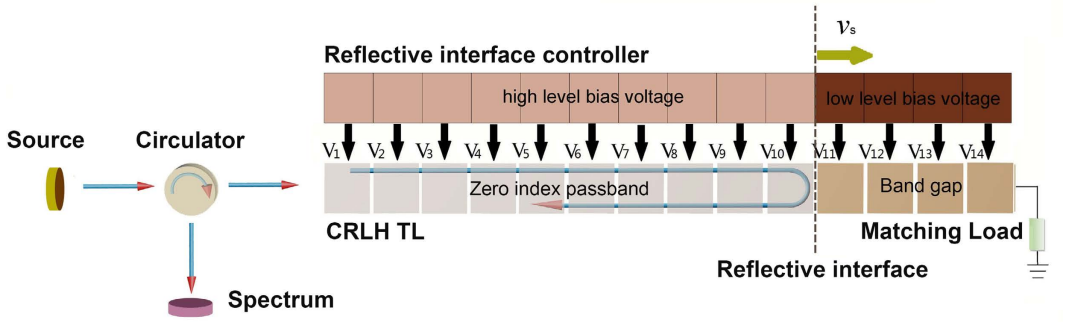

Figure 1. Schematic of the set-up to realize the zero, inverse and normal Doppler Effect. The whole experimental set-up. $V_i(i = 1, 2 \ldots 14)$ are the bias voltages provided to the CRLH TL units. The TL units in gray are set in zero-index passband (can also be LH, RH at different frequencies) while units in dark brown are set in band gap. v_s is the moving velocity of the reflective interface.

unit. Depending on the time interval of the alternation of adjacent units' bias voltages, the moving velocity of the reflective interface v_s can be varied through the reflective interface controller. The RF signal is injected through a circulator into this CRLH transmission line when the passband is set at zero-index point as shown in Fig. 1.

Results

Characteristics of the tunable composite right-left handed transmission line. The unit of the composite right-left handed transmission line is composed of microstrip line loaded with two 19 pF capacitors in series and one varactor NXP BB131 in parallel, as shown in Fig. 2a. Once the bias voltages changes, the capacitances of the varactor would vary - leading to the variation of dispersion curve. The theoretical dispersion curve of the transmission line can be computed by using ABCD matrixes (See details in Supplementary Text). The relative permittivity and permeability are:

$$\varepsilon_r = \frac{1}{pd\varepsilon_0}\left(3C_R d_1 - \frac{1}{\omega^2 L} + \frac{C_0(\omega^2 L_R C_R d_1^2 - 1)}{\omega^2 L_R C_R d_1^2 - 1 + \omega^2 L_R C_0 d_1}\right) \quad (1)$$

$$\mu_r = \frac{p}{d\mu_0}\left(3L_R d_1 - \frac{2}{\omega^2 C}\right) \quad (2)$$

where p, the structure constant, is 4.05 in our case. ε_0, μ_0 are permittivity and permeability in vacuum separately. C_R, L_R are the distributed capacitance and inductance of the transmission line, C, C_0 are the capacitance of the loaded series capacitor and the varactor separately. d, d_1 are the lengths of unit and the microstrip line shown in Fig. 2a, see details in Methods.

The capacitance of the varactor C_0, will vary with the bias voltage. Therefore, by choosing a proper series capacitor C and bias voltage, one can make both permittivity and permeability near zero, leading to a zero-index transmission line and zero wave vector. Meanwhile, the negative and positive permittivity and permeability can also be obtained by choosing different operating frequencies.

Figure 2b is the comparison between theoretical and experimental dispersion curves of the balanced transmission line. The inset is the zoom-in of the linear dispersion at zero-index frequency which is emphasized in a green ellipse. The experimental zero-index frequency is achieved at $f_Z = 852\,\mathrm{MH_Z}$, slightly lower than the theoretical one $f_{Z'} = 879\,\mathrm{MH_Z}$. The phase velocity is shown in Fig. 2c, which turns to be very large at the zero-index frequency. The propagation of wave at f_Z inside the transmission line is shown in Supplementary Movie 1, in which one can see there is no phase variation inside the CRLH TL, while the energy keeps flowing through it.

Figure 2d illustrates the experimental transmission characteristics (in terms of $|S_{21}|$) of the CRLH transmission line under two bias voltages of 16 V (red solid line) and 0 V (blue dotted line). We can see that the transmission sustains across a wide frequency band, covering left-handed region, zero-index frequency and right-handed region when the transmission line is balanced under 16 V bias voltage (see Supplementary Fig. 2b). There is around 10 dB loss, which is mainly due to the reflection at the input port (see Supplementary Fig. 3b). When the bias voltages are turned off to 0 V, the capacitance of the varactors increases and the original passband becomes a band gap (stopband). Therefore, a reflective interface can be formed between units set in passbands (16 V) and band gap (0 V).

Theoretical Doppler frequency shifts. As a unique character of zero-index metamaterial, electromagnetic wave inside such ZIM has an infinite long wavelength, exhibiting a constant spatial distribution that varies temporally while propagating through the ZIM (see details in Supplementary Text and Movie 1)[25], resulting in that the detector can not "sense" any compression or stretch of the wave front. As a result, the zero Doppler effect can be observed under this condition.

The Doppler effect can be governed by the following equation between the frequencies of the incident wave f_i and reflected wave f_r^2:

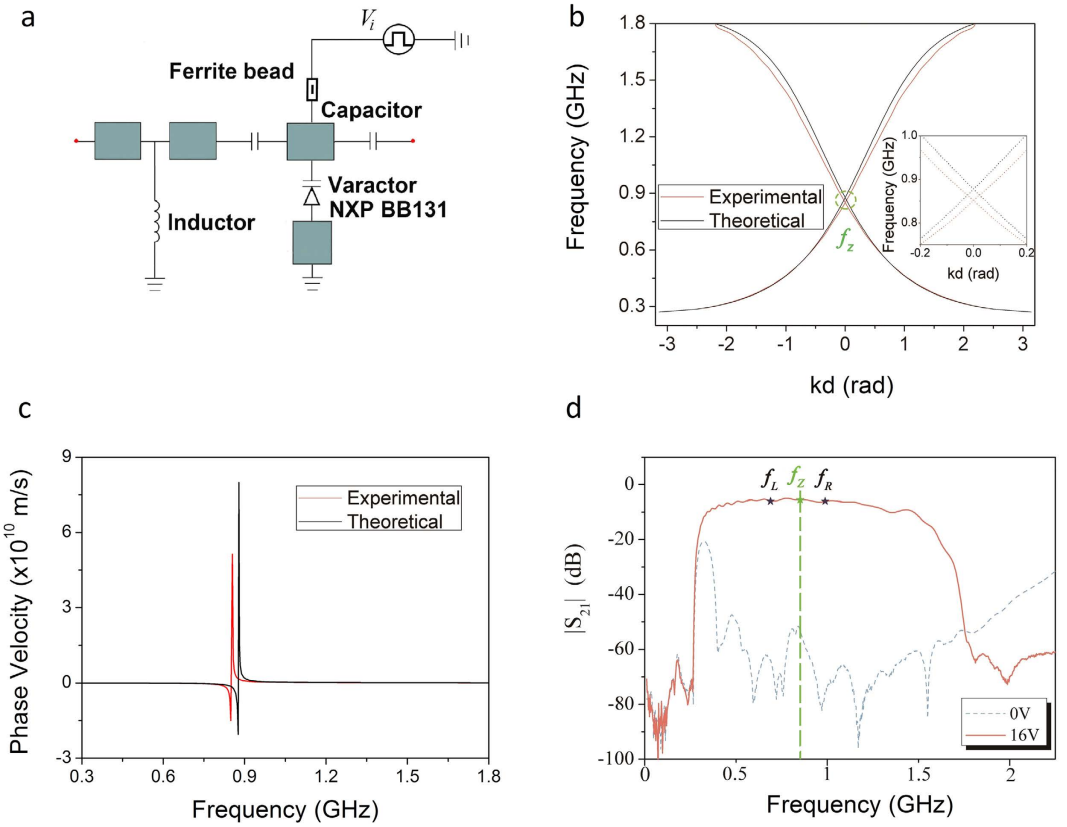

Figure 2. Transmission characteristics of the transmission under different bias voltages. (**a**) Schematic of the CRLH TL unit. See more details in Methods and Supplementary Text. (**b**) The theoretical dispersion curves derived by ABCD matrix method and experimental dispersion curves of the balanced CRLH TL, the inset is the zoom-in of curves inside the green ellipse. f_Z is the experimental (near) zero-index frequency 852 MHz. (**c**) The theoretical and experimental phase velocities obtained from Fig. 2b. (**d**) $|S_{21}|$ of the CRLH TL under 16 V (red solid lines) and under 0 V (blue dotted line). f_L, f_R are frequencies 690 MHz and 990 MHz specifically. The former is frequency set in left-handed passband while the latter is set in right-handed passband. Green dotted line indicates the zero-index frequency.

$$\frac{f_r}{f_i} = \frac{1 - (\vec{v}_m \cdot \vec{v}_i)/v_i^2}{1 - (\vec{v}_m \cdot \vec{v}_r)/v_r^2} \tag{3}$$

where $\vec{v}_m$, $\vec{v}_i$, $\vec{v}_r$ are the velocities of the moving reflective interface, incident wave and reflected wave separately. The velocities are positive when moving away from the source. In our work, the phase velocities of the incident and reflected wave are near equal ($|\vec{v}_i| \approx |\vec{v}_r|$) in the range of Doppler shifts (see more in the Supplementary Text).

At the zero-index frequency f_z, the refractive index and propagation constant are both close to zero. Hence the phase velocity at f_z is infinite according to its definition ($v_p = \frac{c}{n} = \frac{c}{\sqrt{\varepsilon_r \mu_r}}$, where c is the wave speed in free space), shown in Fig. 2c. Therefore, equation (3) falls to:

$$\frac{f_r}{f_i} \to 1 \tag{4}$$

when $f_i = f_z$.

Equation (4) shows that the reflected signal frequency would always keep the same with the incident signal frequency, no matter how fast the reflective interface moves, which is called the zero Doppler effect.

Measured zero Doppler shifts. In order to demonstrate the zero Doppler effect in experiment, the spectra of the reflected signal with incident frequencies near the zero-index frequency are displayed in Fig. 3. Spectra at left side are under the condition that the reflective interface is approaching the source at four different velocities, while the ones at right side are under the condition that the reflective interface is receding at the same speed as the left ones.

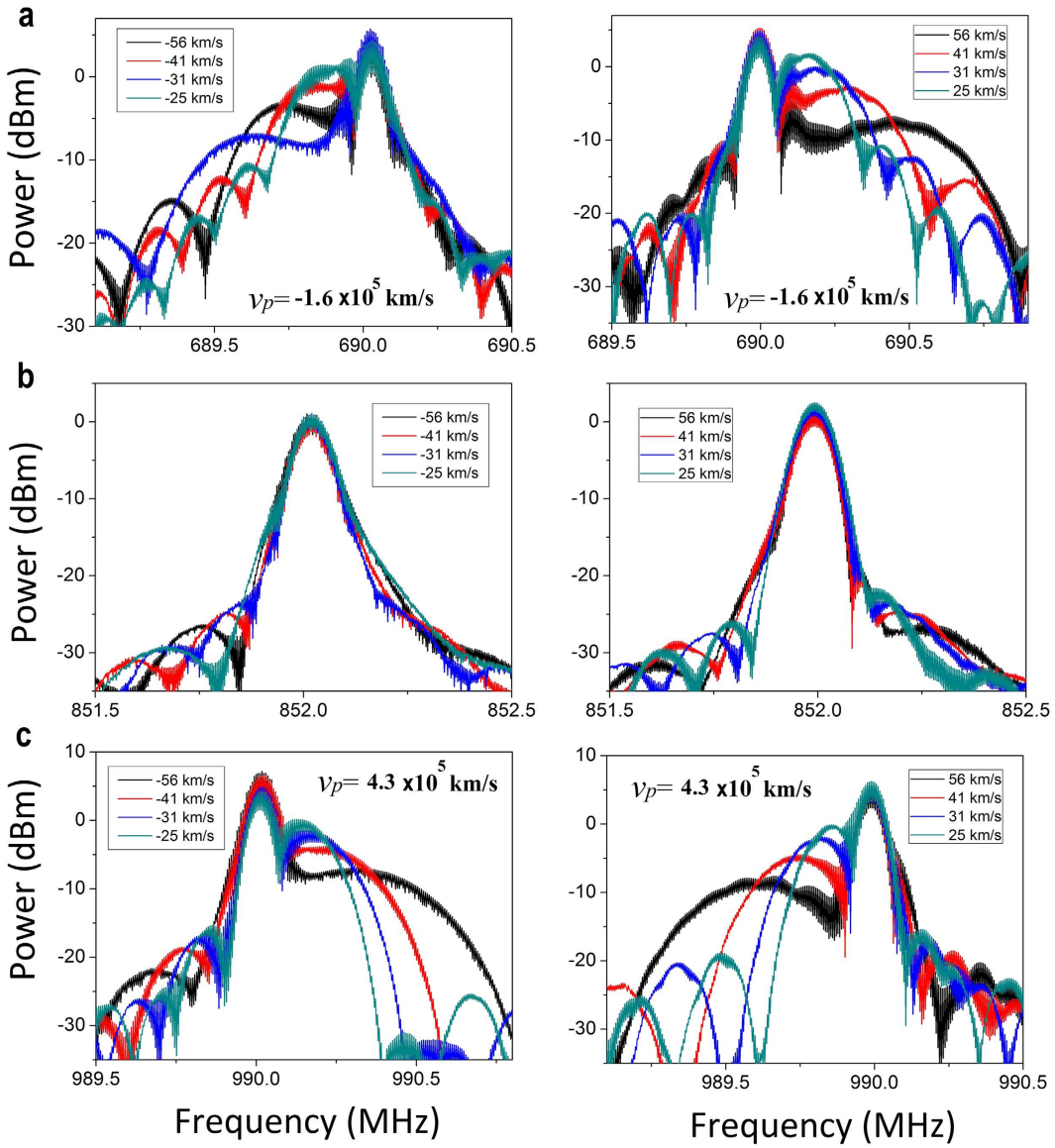

Figure 3. Spectra of the experimental inverse, zero and normal Doppler effects. (**a**–**c**) Spectra of the reflected wave at three frequencies: (**a**) $f_L = 690\,\mathrm{MH_Z}$, (**b**) $f_Z = 852\,\mathrm{MH_Z}$, and (**c**) $f_R = 990\,\mathrm{MH_Z}$ with the same speed of the reflective interface. The spectra at left side are under the condition that the interface is approaching the source while the spectra at right side are under the condition that the interface is moving away from the source.

When the incident frequency is set either below the zero-index frequency ($f_L = 690\,\mathrm{MH_Z}$) in Fig. 3a or above the zero-index frequency ($f_R = 990\,\mathrm{MH_Z}$) in Fig. 3c, there appear two major peaks on the spectra at each velocity of the reflective interface: the higher peak corresponding to the incident frequency owing to the reflection at the input port, while the lower peak corresponding to the frequency of shifted components, i.e. the (inverse) Doppler shifts. However, when the signal is injected into the CRLT transmission line at the zero-index frequency ($f_Z = 852\,\mathrm{MH_Z}$) in Fig. 3b, there only appear one major peak on the spectra, corresponding to the incident frequency, irrespective of the motion of the reflective interface. As a result, we can conclude that zero Doppler shift was observed at the zero-index frequency.

Figure 4 shows a complete picture of the Doppler effects (normal, inverse and zero shifts) when the EM wave travels in this balanced transmission line, depending on the moving velocity of the reflective interface and frequency. The surface is the theoretical result computed by using Equation (3) while the lines with markers are measured ones (yellow, green are the inverse, normal Doppler shifts separately). Line a and c are the measured inverse and normal Doppler shifts at 570 MHz and 1.07 GHz specifically, whose spectrum are shown in Supplementary Fig. 6. The near zero frequency shifts at zero-index frequency are observed in the resolution of 0.2 MHz, denoted by red dotted line b. We can see that the surface is twisted around the zero-index frequency

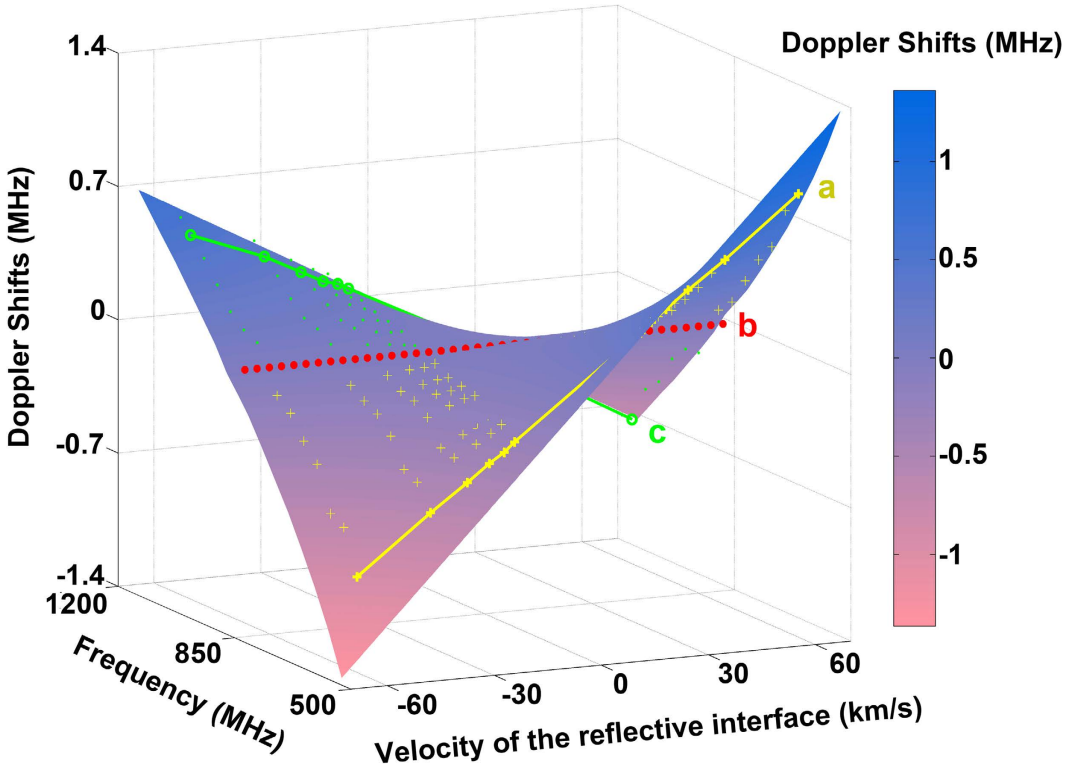

Figure 4. Comparison between the theoretical and experimental Doppler shifts. The surface is the theoretical shifts based on Equation (3) while the markers are experimental shifts, with yellow cross-shaping markers as inverse Doppler shifts and green dots as normal Doppler shifts. Lines a, c are experimental shifts picked to underline the inverse and normal Doppler shifts separately. Line b is the measured zero Doppler shifts in the resolution of 0.2 MHz.

and the theoretical slope of line b at 852 MHz is near zero, which means that, no matter which direction ($v_s > 0$ or $v_s < 0$) and how fast the reflective interface moves, there would be no frequency shift. That is what we called zero Doppler effect.

Discussion

The zero Doppler effect is observed for the first time in experiment on a zero-index metamaterial based on a tunable composite right/left-handed transmission line loaded with the varactors. As a unique character of the zero-index material, the wave propagates through it without any phase change, leading to neither phase compression, nor phase stretch when there is a relative motion between the signal and the detector. As a result, there would be no Doppler shift no matter how the relative motion is.

The most crucial parts of our experiment are the realization of the zero-index metamaterial and the formation of reflective interface on this CRLH transmission line, which can move at a certain velocity controlled by an electrical circuit, leading to a relative motion between the source and the detector. The normal Doppler effect or the inverse Doppler effect can also be realized on the CRLH transmission line when the incident frequency falls into the right-handed passband or the left-handed passband respectively. The maximal frequency shift is mainly limited by the performances of the components on the digital switching circuit, which lead to the finite rising and falling edges (~10 ns for each) of the pulse signal. As a result, the internal of the bias voltages' rising or falling edges would be no shorter than 20 ns. Utilizing high performance components can therefore increase the maximal Doppler shift and the resolution. It is worth mentioning that zero Doppler effect observed in the zero-index metamaterials is different from the concept of 'zero Doppler effect' in radar technology, which stands for a technique to compensate the normal Doppler frequency shift. The wave in the near zero-index medium has been shown no frequency shifts irrespective of the relative motion between the source and the detector. It is expected that our work may attract more research interest in exploiting zero-index metamaterials and lead to potential applications in EM wave related metrology.

Methods

Fabrication of the 1D tunable composite right-left handed transmission line (CRLH TL). The tunable composite right/left-handed transmission line (CRLH TL) is fabricated on the FR4 dielectric slab with permittivity $\varepsilon_r = 4.75$, thickness $h = 1.6\,mm$. The microstrip lines are made of copper with width $w = 3\,mm$, lengths $d_1 = 3.6\,mm$, $d_2 = 1.8\,mm$. The unit of the transmission line is loaded with two capacitors $C = 19$ pF in

series, one inductance $L = 10$ nH and a varactor BB131 in parallel. The distributed capacitance and inductance are $C_R = 1.2789 \times 10^{-10}$ F and $L_R = 3.1978 \times 10^{-7}$ H. The varactor is connected to the ground via hole. Total length of the unit is $d = 12.37$ mm, shown in Supplementary Fig. 1a.

Setting up of the CRLH TL, inverse and normal Doppler shift measurements. The Agilent network analyzer N5222A is used to test the transmission characteristic of the composite right-left handed transmission line. All the units of the CRLH TL are supplied the same bias voltage in this test. The set-up for observation of inverse Doppler shifts, shown in Fig. 1, is composed by the Agilent vector signal generator E8267D, a circulator with isolation 20 dB, the Agilent signal analyzer N9020A, the 1D tunable CRLH TL, a 50 Ω matching load and the reflective surface controller. The *Gate* function of the spectrum analyzer is used to select certain time domain when the zero/inverse/normal Doppler shift is happening by inputting the voltage signal of the first unit of the reflective surface controller to the analyzer as the trigger signal and setting the duration of the inverse Doppler shift as the length of the *Gate* function.

References

1. Veselago, V. G. The electrodynamics of substances with simultaneously negative values of permittivity and permeability. *Sov. Phys. Usp*. **10,** 509–514 (1968).
2. Seddon, N. & Bearpark, T. Observation of the inverse Doppler effect. *Science* **302,** 1537–1540 (2003).
3. Ran, J. *et al.* Realizing tunable inverse and normal Doppler shifts in reconfigurable RF metamaterials. *Sci. Rep.* **5,** 11659 (2015).
4. Chen, J. B. *et al.* Observation of the inverse Doppler effect in negative-index materials at optical frequencies. *Nature Photon*. **5,** 239–242 (2011).
5. Hu, X. H., Hang, Z. H., Li, J., Zi, J. & Chan, C. T. Anomalous Doppler effects in phononic band gaps. *Phys. Rev. E* **73,** 015602 (2006).
6. Stancil, D. D., Henty, B. E., Cepni, A. G. & Van't Hof, J. P. Observation of an inverse Doppler shift from left-handed dipolar spin waves. *Phys. Rev. B* **74,** 060404 (2006).
7. Chumak, A. V., Dhagat, P., Jander, A., Serga, A. A. & Hillebrands, B. Reverse Doppler effect of magnons with negative group velocity scattered from a moving Bragg grating. *Phys. Rev. B* **81,** 140404 (2010).
8. Belyantsev, A. M. & Kozyrev, A. B. Generation of RF oscillations in the interaction of an electromagnetic shock with a synchronous backward wave. *Tech. Phys.* **45,** 747–752 (2000).
9. Leong, K. M. K. H., Lai, A. & Itoh, T. Demonstration of reverse Doppler effect using a left-handed transmission line. *Microw. Opt. Technol. Lett*. **48,** 545–547 (2006).
10. Pendry, J. B. Negative refraction makes a perfect lens. *Phys. Rev. Lett.* **85,** 3966–3969 (2000).
11. Smith, D. R., Padilla, W. J., Vier, D. C., Nemat-Nasser, S. C. & Schultz, S. Composite medium with simultaneously negative permeability and permittivity. *Phys. Rev. Lett.* **84,** 4184–4187 (2000).
12. Shelby, R. A., Smith, D. R. & Schultz, S. Experimental verification of a negative index of refraction. *Science* **292,** 77–79 (2001).
13. Schurig, D. *et al.* Metamaterial electromagnetic cloak at microwave frequencies. *Science* **314,** 977–980 (2006).
14. Chen, H. S., Wu, B. I., Zhang, B. & Kong, J. A. Electromagnetic wave interactions with a metamaterial cloak. *Phys. Rev. Lett.* **99,** 063903 (2007).
15. Pendry, J. B., Schurig, D. & Smith, D. R. Controlling electromagnetic fields. *Science* **312,** 1780–1782 (2006).
16. Engheta, N. & Ziolkowski, R. W. In *Metamaterials: physics and engineering explorations* (ed. EI-Hawary, M. E. *et al.*) (Wiley-IEEE, 2006).
17. Caloz, C. & Itoh, T. In *Electromagnetic metamaterials transmission line theory and microwave application* (Wiley-IEEE, 2005).
18. Luo, H. L. *et al.* Rotational Doppler effect in left-handed materials. *Phys. Rev. A* **78,** 033805 (2008).
19. Jiang, H. T., Chen, H. & Zhu, S. Y. Rabi splitting with excitons in effective (near) zero-index media. *Opt. Lett.* **32,** 1980–1982 (2007).
20. Hao, J. M., Yan, W. & Qiu, M. Super-reflection and cloaking based on zero index metamaterial. *Appl. Phys. Lett.* **96,** 101109 (2010).
21. Huang, X., Lai, Y., Hang, Z. H., Zheng, H. & Chan, C. T. Dirac cones induced by accidental degeneracy in photonic crystals and zero-refractive-index materials. *Nat. Mater.* **10,** 582–586 (2011).
22. Jiang, H. T. *et al.* Enhancement of (nearly) homogeneous fields in a (effective) zero-index cavity. *J. Appl. Phys.* **109,** 073113 (2011).
23. Li, Y. H. *et al.* Arbitrary angle waveguide bends based on zero-index metamaterials. *Appl. Phys. A* **117,** 1541–1545 (2014).
24. Zhang, C., Chan, C. T. & Hu, X. Broadband focusing and collimation of water waves by zero refractive index. *Sci. Rep*. **4,** 6979 (2014).
25. Ziolkowski, R. W. Propagation in and scattering from a matched metamaterial having a zero index of refraction. *Phys. Rev. E* **70,** 046608 (2004).
26. Caloz, C. & Itoh, T. Novel microwave devices and structures based on the transmission line approach of metamaterials. *IEEE MTT-S Int. Microw. Symp. Dig*. **1,** 195–198 (2003).
27. Eleftheriades, G. V., Iyer, A. K. & Kremer, P. C. Planar negative refractive index media using periodically L-C loaded transmission lines. *IEEE Trans. Microwave Theory Tech*. **50,** 2702–2712 (2002).
28. Caloz, C. & Itoh, T. Application of the transmission line theory of left-handed (LH) materials to the realization of a microstrip "LH line". *IEEE-APS Int. Symp.Dig.* **2,** 412–415 (2002).
29. Iyer, A. K. & Eleftheriades, G. V. Negative refractive index metamaterials supporting 2-D waves. *IEEE MTT-S Int. Microwave Symp. Dig.* **2,** 1067–1070 (2002).
30. Lai, A., Caloz, C. & Itoh, T. Composite right/left-handed transmission line metamaterials. *IEEE Microwave Magazine* **5,** 34–50 (2004).

Acknowledgements

This work is supported by the National Basic Research Program (973) of China (No. 2011CB922001), and National Natural Science Foundation of China (No. 11234010).

Author Contributions

J.R. fabricated the transmission line and conducted the measurements and the simulations; Y.Z. leaded the experiments and simulations; Y.Z. and X.C. discussed the physical mechanism and experimental results; J.Z. and K.F. developed the original reflective surface controller and performed part of the simulation; J.R., Y.Z., X.C., K.F. wrote and modified the manuscript; H.C. suggested important idea and physical mechanism.

Additional Information

Supplementary information accompanies this paper at http://www.nature.com/srep

Competing financial interests: The authors declare no competing financial interests.

How to cite this article: Ran, J. *et al.* Observation of the Zero Doppler Effect. *Sci. Rep.* **6**, 23973; doi: 10.1038/srep23973 (2016).